

Cu NQR and NMR Studies of Optimally Doped $\text{Ca}_{2-x}\text{Na}_x\text{CuO}_2\text{Cl}_2$

Yutaka ITOH*, Takato MACHI¹, Ikuya YAMADA², Masaki AZUMA³, and Mikio TAKANO⁴

Department of Physics, Graduate School of Science, Kyoto Sangyo University, Kamigamo-Motoyama, Kika-ku Kyoto 603-8555, Japan

¹*Superconductivity Research Laboratory, International Superconductivity Technology Center, 1-10-13 Shinonome, Koto-ku Tokyo 135-0062, Japan*

²*Osaka Prefecture University, Sakai, Osaka 599-8531, Japan*

³*Materials and Structures Laboratory, Tokyo Institute of Technology, Nagatsuta, Midori-ku, Yokohama 226-8503, Japan*

⁴*Institute for Chemical Research, Kyoto University, Uji, Kyoto 611-0011, Japan*

KEYWORDS: $\text{Ca}_{2-x}\text{Na}_x\text{CuO}_2\text{Cl}_2$, nuclear quadrupole resonance, NMR, superconductor

Copper oxychloride $\text{Ca}_{2-x}\text{Na}_x\text{CuO}_2\text{Cl}_2$ is a single- CuO_2 -layer system of high- T_c cuprate superconductors.^{1,2} The parent compound $\text{Ca}_2\text{CuO}_2\text{Cl}_2$ is one of the ideal square lattice antiferromagnets with no orthorhombic distortion. Apical chlorine distant from the CuO_2 plane is characteristic of this system. For Na substitution, the crystal symmetry is still tetragonal, and the oxygen and chlorine composition is robust. The flat CuO_2 plane is similar to $\text{HgBa}_2\text{CuO}_{4+\delta}$. The out-of-plane disorder of the Na dopant for the Ca site primarily causes randomness effect. A higher T_c has been associated with the flatness of CuO_2 planes in a unit cell. However, the optimized $T_c \approx 28$ K with $x \approx 0.2$ is lower than the highest $T_c \approx 98$ K of $\text{HgBa}_2\text{CuO}_{4+\delta}$. The single crystals grown at high pressure³ were served for scanning tunneling spectroscopy (STS) studies, which revealed exotic electronic states.⁴⁻⁶

In this note, we report on $^{63,65}\text{Cu}$ nuclear quadrupole resonance (NQR) and NMR studies of an optimally doped superconductor $\text{Ca}_{2-x}\text{Na}_x\text{CuO}_2\text{Cl}_2$ ($T_c \approx 28$ K for $x \approx 0.2$). Although the system has a robust oxygen composition, we observed a multiple Cu NQR frequency spectrum and broad Cu NMR spectra. We also observed nonexponential nuclear spin-lattice relaxation. Some inhomogeneous features are similar to those for $\text{La}_{2-x}\text{Sr}_x\text{CuO}_{4-\delta}$.

A polycrystalline sample of $\text{Ca}_{1.8}\text{Na}_{0.2}\text{CuO}_2\text{Cl}_2$ was synthesized under high pressure, as described in refs. 1 and 2. The sample was confirmed to be in the single phase from its powder X-ray diffraction pattern. For the NMR and NQR experiments, the grains of the powder were aligned in a magnetic field of about 8 T and were fixed in an epoxy resin (Staycast 1266).⁷

A phase-coherent-type pulsed spectrometer was utilized to perform the $^{63,65}\text{Cu}$ NQR and NMR (nuclear spin $I = 3/2$) experiments for the c -axis-aligned sample. The spectra were obtained by recording the spin-echo intensity against frequency point by point. Cu nuclear spin-lattice relaxation curves $p(t) \equiv 1 - M(t)/M(\infty)$ (recovery curves) were mea-

sured by an inversion recovery technique as a function of time t after an inversion pulse, where the nuclear spin-echo $M(t)$, $M(\infty)[\equiv M(10T_1)]$, and t were recorded.

The recovery curves in the Cu NQR were analyzed by an exponential function with T_1 multiplied by a stretched exponential function with τ_1 , $p(t) = p(0)e^{-3t/T_1 - \sqrt{3t/\tau_1}}$, as in refs. 8 and 9. The finite $1/\tau_1$ indicates the existence of random relaxation centers, e.g., local moments of dilute magnetic impurities, and spinless defects in strongly correlated systems. T_1 is due to the host electron spin relaxation process.

Figure 1 shows the zero field $^{63,65}\text{Cu}$ NQR frequency spectrum at $T = 4.2$ K. Solid and dashed curves are guides for the eye showing Gaussian functions. A pair of $^{63,65}\text{Cu}$ isotope NQR signals is assigned to a Cu site. The natural abundance ratio of the two $^{63,65}\text{Cu}$ isotopes is 0.69:0.31. The quadrupole moment ratio of the two $^{63,65}\text{Cu}$ isotopes is $^{63}Q/^{65}Q = 1.08$. A pair of Gaussian functions with the relevant intensity and resonance frequency ratios is assumed for a Cu site. In Fig. 1, two Cu sites are assumed to reproduce the observed NQR spectrum, although the decomposition is not unique.

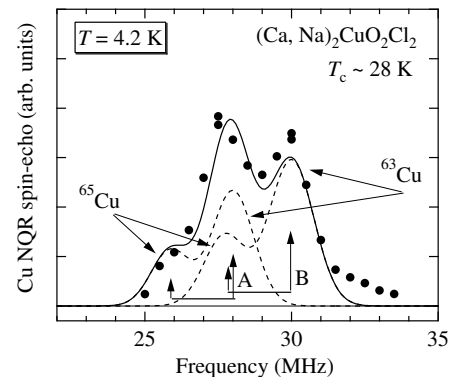


Fig. 1. Zero-field Cu NQR spectrum (solid circles) of $\text{Ca}_{2-x}\text{Na}_x\text{CuO}_2\text{Cl}_2$ ($T_c \approx 28$ K, $x \approx 0.2$) at $T = 4.2$ K. Dashed curves are guides for the eye showing double Gaussian functions for a pair of $^{63,65}\text{Cu}$ isotopes. A solid curve is a simulation with the ^{63}Cu peaks at $f_A = 28.0$ MHz and $f_B = 30.0$ MHz.

The multiple features are similar to those for $\text{La}_{2-x}\text{Sr}_x\text{CuO}_{4-\delta}$ ¹⁰⁻¹³ and $\text{La}_2\text{CuO}_{4+\delta}$.¹⁴ Randomness in crystalline potentials is not sufficient to cause such a multiple NQR spectrum.^{15,16} Some modulation in the charge density of the CuO_2 planes may be induced by the doped holes. The symmetry of the charge density may be broken to become lower than the tetragonal symmetry of the original square lattice. The electronic cluster glass in the STS observation⁵ is such a misfit state, and can cause the multiple broad Cu NQR spectrum.

Figure 2 shows temperature dependences of Cu nuclear spin-lattice relaxation rates of the Cu NQR ($f_A = 28.0$ MHz) for $\text{Ca}_{1.8}\text{Na}_{0.2}\text{CuO}_2\text{Cl}_2$, (a) the stretched exponential relaxation rate $1/\tau_1$ and (b) the exponential relaxation rate divided by T , $1/T_1T$. For comparison, $1/\tau_1$ and $1/T_1T$ for $\text{La}_{2-x}\text{Sr}_x\text{CuO}_{4-\delta}$ ($x = 0.13$ and 0.18)⁹ and for $\text{HgBa}_2\text{CuO}_{4+\delta}$ ($T_c = 96$ K)^{17,18} are also shown.

In Fig. 2(a), $1/\tau_1$ of $\text{Ca}_{1.8}\text{Na}_{0.2}\text{CuO}_2\text{Cl}_2$ is similar to those of $\text{La}_{2-x}\text{Sr}_x\text{CuO}_{4-\delta}$. The appreciable $1/\tau_1$ indicates the existence of a slow fluctuation mode in a low-frequency spin fluctuation spectrum, which could cause the pair-breaking effect.^{8,9} The electronic cluster glass state⁵ can be the low-frequency local modes.⁹

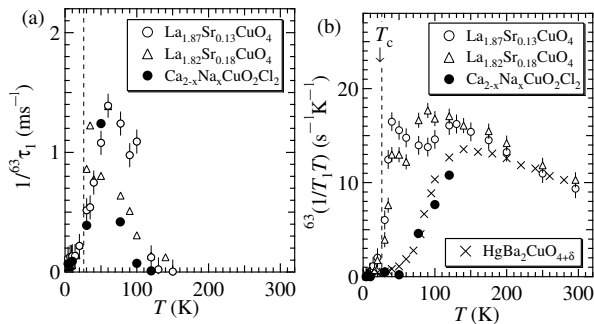


Fig. 2. Temperature dependences of Cu nuclear spin-lattice relaxation rates $1/\tau_1$ (a) and $1/T_1T$ (b) at $f_A = 28.0$ MHz for $\text{Ca}_{1.8}\text{Na}_{0.2}\text{CuO}_2\text{Cl}_2$. $1/\tau_1$ and $1/T_1T$ (open circles and open triangles) of ^{63}Cu (A) of $\text{La}_{2-x}\text{Sr}_x\text{CuO}_{4-\delta}$ ($x = 0.13$ and 0.18) are reproduced from ref. 9. $1/T_1T$ of ^{63}Cu of optimally doped $\text{HgBa}_2\text{CuO}_{4+\delta}$ ($T_c = 96$ K) is reproduced from refs. 17 and 18.

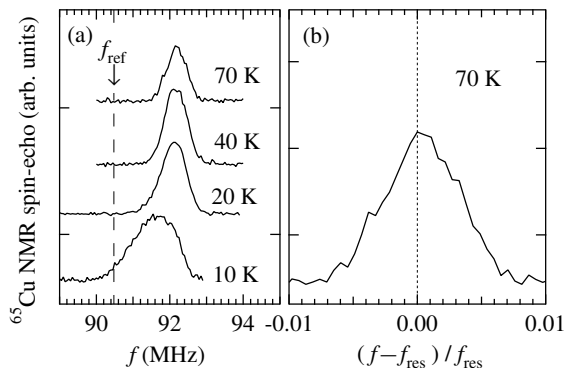


Fig. 3. (a) Temperature dependence of central transition lines ($I_z = 1/2 \leftrightarrow -1/2$) of ^{63}Cu NMR frequency spectra for $\text{Ca}_{1.8}\text{Na}_{0.2}\text{CuO}_2\text{Cl}_2$ in a magnetic field of 7.48414 T along the c axis. $f_{\text{ref}} = 90.4758$ MHz denotes the zero shift resonance frequency. (b) ^{63}Cu NMR spectrum at 70 K against the normalized frequency shift defined by $(f - f_{\text{res}})/f_{\text{res}}$ with $f_{\text{res}} = 92.15$ MHz.

In contrast to the random relaxation process of $1/\tau_1$, the uniform relaxation process of $1/T_1T$ for $\text{Ca}_{1.8}\text{Na}_{0.2}\text{CuO}_2\text{Cl}_2$ is different from those of $\text{La}_{2-x}\text{Sr}_x\text{CuO}_{4-\delta}$, but similar to that of the optimally doped $\text{HgBa}_2\text{CuO}_{4+\delta}$ ($T_c = 96$ K).

Figure 3(a) shows the central transition lines ($I_z = 1/2 \leftrightarrow -1/2$) of ^{63}Cu NMR frequency spectra for $\text{Ca}_{1.8}\text{Na}_{0.2}\text{CuO}_2\text{Cl}_2$ in a magnetic field of 7.48414 T applied along the c axis. We

focused on ^{65}Cu NMR experiments, because the nuclear gyromagnetic ratio $^{65}\gamma_n$ of ^{65}Cu is close to that of ^{23}Na , making their NMR signals indistinguishable. The ^{65}Cu NMR spectrum was nearly independent of temperature. The Knight shift

$^{65}K_{\text{cc}}$ was estimated to be $\sim 1.85\%$ in the temperature range of 20–100 K.

The NMR linewidth at $T = 10$ K is broader than those above 20 K. This is due to the distribution of local internal fields of a vortex lattice in the mixed state of the type II superconductor. The vortex pattern is unclear in the present NMR line profile; hence it might be due to a Bragg glass.

Figure 3(b) shows the ^{65}Cu NMR spectrum at 70 K against the normalized frequency shift defined by $(f - f_{\text{res}})/f_{\text{res}}$ with the peak frequency f_{res} . The broad linewidth of $\text{Ca}_{1.8}\text{Na}_{0.2}\text{CuO}_2\text{Cl}_2$ is about 5 times wider than that of $\text{HgBa}_2\text{CuO}_{4+\delta}$ ¹⁸ and is also observed for $\text{La}_{2-x}\text{Sr}_x\text{CuO}_{4-\delta}$.¹⁹ Thus, a common electronic inhomogeneity is observed in $\text{Ca}_{1.8}\text{Na}_{0.2}\text{CuO}_2\text{Cl}_2$ and $\text{La}_{2-x}\text{Sr}_x\text{CuO}_{4-\delta}$.^{9,12,13,19}

Acknowledgments We thank K. Oka for experimental support. Y. I. thanks H. Kageyama for sample preparation at an early stage. This study was supported in part by Grant-in-Aid for Scientific Research (C), from the Ministry of Education, Culture, Sports, Science and Technology of Japan (Grant No. 22540353).

- 1) Z. Hiroi, N. Kobayashi, and M. Takano: Nature (London) **371** (1994) 139.
- 2) Z. Hiroi, N. Kobayashi, and M. Takano: Physica C **266** (1996) 191.
- 3) M. Azuma, T. Saito, I. Yamada, Y. Kohsaka, H. Takagi, and M. Takano: J. Low Temp. Phys. **131** (2003) 671.
- 4) T. Hanaguri, C. Lupien, Y. Kohsaka, D.-H. Lee, M. Azuma, M. Takano, H. Takagi, and J. C. Davis: Nature **430** (2004) 1001.
- 5) Y. Kohsaka, C. Taylor, K. Fujita, A. Schmidt, C. Lupien, T. Hanaguri, M. Azuma, M. Takano, H. Eisaki, H. Takagi, S. Uchida, and J. C. Davis: Science **315** (2007) 1380.
- 6) T. Hanaguri, Y. Kohsaka, J. C. Davis, C. Lupien, I. Yamada, M. Azuma, M. Takano, K. Ohishi, M. Ono, and H. Takagi: Nature Phys. **3** (2007) 865.
- 7) M. Takigawa, P. C. Hammel, R. H. Heffner, Z. Fisk, J. L. Smith, and R. B. Schwarz: Phys. Rev. B **39** (1989) 300.
- 8) Y. Itoh, T. Machi, C. Kasai, S. Adachi, N. Watanabe, N. Koshizuka, and M. Murakami: Phys. Rev. B **67** (2003) 064516.
- 9) Y. Itoh, T. Machi, N. Koshizuka, M. Murakami, H. Yamagata, and M. Matsumura: Phys. Rev. B **69** (2004) 184503.
- 10) K. Yoshimura, T. Imai, T. Shimizu, Y. Ueda, K. Kosuge, and H. Yasuoka: J. Phys. Soc. Jpn. **58** (1989) 3057.
- 11) K. Yoshimura, T. Uemura, M. Kato, K. Kosuge, T. Imai, and H. Yasuoka: Hyperfine Interactions **79** (1993) 867.
- 12) P. M. Singer, A. W. Hunt, and T. Imai: Phys. Rev. Lett. **88** (2002) 047602.
- 13) P. M. Singer, T. Imai, F. C. Chou, K. Hirota, M. Takaba, T. Kakeshita, H. Eisaki, and S. Uchida: Phys. Rev. B **72** (2005) 014537.
- 14) P. C. Hammel, A. P. Reyes, S.-W. Cheong, Z. Fisk, and J. E. Schirber: Phys. Rev. Lett. **71** (1993) 440.
- 15) Y. Itoh, S. Adachi, T. Machi, and N. Koshizuka: Phys. Rev. B **64** (2001) 180511.
- 16) G. V. M. Williams: Phys. Rev. B **76** (2007) 094502.
- 17) Y. Itoh, T. Machi, A. Fukuoka, K. Tanabe, and H. Yasuoka: J. Phys. Soc. Jpn. **65** (1996) 3751.
- 18) Y. Itoh, T. Machi, S. Adachi, A. Fukuoka, K. Tanabe, and H. Yasuoka: J. Phys. Soc. Jpn. **67** (1998) 312.
- 19) Y. Itoh, M. Matsumura, and H. Yamagata: J. Phys. Soc. Jpn. **65** (1996) 3747.